International Journal of Greenhouse Gas Control 38 (2015) 210–220

Contents lists available at ScienceDirect

International Journal of Greenhouse Gas Control

journal homepage: www.elsevier.com/locate/ijggc

Modelling large-scale CO_2 leakages in the North Sea

Jack J.C. Phelps[a,*], Jerry C. Blackford[b], Jason T. Holt[a], Jeff A. Polton[a]

[a] National Oceanography Centre, Joseph Proudman Building, 6 Brownlow Street, Liverpool L3 5DA, UK
[b] Plymouth Marine Laboratory, Prospect Place, Plymouth PL1 3DH, UK

ARTICLE INFO

Article history:
Available online 25 November 2014

Keywords:
Carbon capture and storage
CCS
North Sea
CO_2
Shelf sea
pH

ABSTRACT

A three dimensional hydrodynamic model with a coupled carbonate speciation sub-model is used to simulate large additions of CO_2 into the North Sea, representing leakages at potential carbon sequestration sites. A range of leakage scenarios are conducted at two distinct release sites, allowing an analysis of the seasonal, inter-annual and spatial variability of impacts to the marine ecosystem.

Seasonally stratified regions are shown to be more vulnerable to CO_2 release during the summer as the added CO_2 remains trapped beneath the thermocline, preventing outgasing to the atmosphere. On average, CO_2 injected into the northern North Sea is shown to reside within the water column twice as long as an equivalent addition in the southern North Sea before reaching the atmosphere.

Short-term leakages of 5000 tonnes CO_2 over a single day result in substantial acidification at the release sites (up to -1.92 pH units), with significant perturbations (greater than 0.1 pH units) generally confined to a 10 km radius. Long-term CO_2 leakages sustained for a year may result in extensive plumes of acidified seawater, carried by major advective pathways. Whilst such scenarios could be harmful to marine biota over confined spatial scales, continued unmitigated CO_2 emissions from fossil fuels are predicted to result in greater and more long-lived perturbations to the carbonate system over the next few decades.

1. Introduction

Carbon dioxide capture and storage (CCS) provides the only methodology able to transform fossil fuel based power generation (and some other industrial processes) to relatively low carbon emissions, consistent with climate change mitigation. However, leakage from storage is possible and it is necessary to understand the outcome of a range of leakage scenarios, to enable both efficient monitoring and to understand the nature of environmental impact that could occur.

With little evidence to draw upon, leakage scenarios are somewhat hypothetical, ranging from leakage via abandoned boreholes, leakage through fractures or seismic chimneys and finally catastrophic blowouts. The leakage rate for these scenarios can be estimated as 1, 100–1000 and 10,000 tonnes of CO_2 per day (IEAGHG, 2009), although there is much debate, as yet unpublished, regarding the geological mechanisms that would allow the high end-scenarios. A further set of scenarios can be based on failure of pipeline transport and can be more accurately estimated from existent flow capacities (for example 1 Mt/year or 2740 t/day at Sleipner (Statoil, 2013). Although regulations for CCS pipelines are not finalised, it is industry standard for the oil and gas industry for pipelines to include emergency shutdown values which can close a pipeline instantaneously once a critical threshold of pressure is reached (National Research Council (U.S.), Committee on the Safety of Marine Pipelines, 1994). Once shutdown has occurred rapid depressurisation will occur, depending on the size of the leakage, thus significant leakage can be presumed to be a short-term event of the order of a day. Within this work we do not address the likelihood of leakage, except to make the broad statement that effective monitoring and site operation should render the high end reservoir leakage scenarios highly unlikely to occur.

Given the spatial and temporal scales of impact, no one model system is capable of effectively addressing all possible scenarios; the low-end scenarios result in metre scale impacts (Dewar et al., 2013), whilst the higher end scenarios result in kilometre scale impacts (Blackford et al., 2008). In this paper we investigate the high-end leakage scenarios, with a state of the art three dimensional shelf hydrodynamic model POLCOMS (Holt and James, 2001) coupled with a model of CO_2 speciation in seawater (Blackford and Gilbert, 2007). This allows the assessment of CO_2 plume dispersion within a realistic simulation of the mixing processes that operate in the region. Whilst similar to previously published simulations (Blackford et al., 2008) this work includes improvements to the parameterisation of alkalinity (Artioli et al., 2012), includes density effects associated with high concentrations of CO_2 (Song et al.,

* Corresponding author. Tel.: +44 151 795 4800.
E-mail address: jack.phelps@liverpool.ac.uk (J.J.C. Phelps).

http://dx.doi.org/10.1016/j.ijggc.2014.10.013

2002), has improved assumptions regarding the initial shape of the gaseous CO_2 plume and most importantly provides an order of magnitude increase in model resolution, such that the length scales of model and impact are more consistent. The leakage scenarios in the two studies also differ, and the current investigation explores inter-annual variability.

Addressing these large and arguably highly unlikely scenarios may be seen as unnecessary or alarmist. It is however important to understand the absolute maximum limits on impact that might arise and to underline the need for good operational practice and monitoring. It is also important to understand whether such events are readily detectable.

2. Methodology

2.1. Leakage sites selection

Two locations in the North Sea were selected for the simulated release of CO_2, hereby referred to as the north site (57.75 N, 1.0 E) and the south site (54.0 N, 1.0 E), displayed in Fig. 1. Both of these locations correspond to potential sites of carbon sequestration but differ markedly in the hydro-physical properties. The north site corresponds to the approximate location of the Forties oil field and is characteristic of the relatively deep northern North Sea with a depth of 98 m, whilst the south site represents the approximate location of the Viking group of oil fields and is more typical of the shallow southern North Sea with a depth of 43 m. These locations also correspond with earlier work (Blackford et al., 2008) but with improved estimates of bathymetry.

Both stations experience strong macro-tidal flow, with spring tidal velocities reaching approximately 0.5 m/s and 0.85 m/s at the north and south site, respectively. Mean residual circulation at the north site is dominated by the Dooley Current, a broad semi-permanent barotropic current that flows eastwards, following the meandering 100-m isobath (Svendsen et al., 1991; Holt and Proctor, 2008). Although the Dooley Current reaches speeds of 0.3 m/s, the north site is some distance from these peak flows, and bottom velocities are somewhat weaker. POLCOMS model output suggests that there is a considerable degree of spatial variability to the mean circulation at the south site, and the mean flow is an order of magnitude weaker than the tidal currents. The mean residual circulation in the North Sea is displayed in Fig. 2.

Stratification in the North Sea is predominantly controlled by temperature, with the exception of the Norwegian Trench and the southern coastal regions near large continental rivers, where freshwater inputs result in salinity stratification (Holt and Proctor, 2008). Seasonal surface heat fluxes lead to strong stratification in the northern North Sea during the summer, with surface to bottom temperature differences exceeding 10 °C, whilst the shallower waters further south remain vertically mixed throughout the year (Fig. 1b). The vertical temperature structure at the two sites investigated here broadly reflect this pattern, surface to bottom temperature differences at the north site reach 8.7 °C, although the south site actually lies in a transitional region and does experience some weak stratification for short periods of time (Fig. 3). For a more thorough account of the physical oceanography of the North Sea, the reader is referred to Svendsen et al. (1991).

2.2. Model description

The hydrodynamic component of this modelling study is provided by POLCOMS and is fully described in Holt and James (2001) and Holt and Proctor (2008). POLCOMS is a three dimensional hydrodynamic model formulated upon a staggered Arakawa B-grid (Arakawa and Lamb, 1977) in the horizontal, and terrain following σ-coordinates in the vertical. The model uses the piecewise parabolic method (PPM) advection scheme (Colella and Woodward, 1984), favoured for being highly non-diffusive (James, 1996). The combination of the B-grid and the advection scheme ensure POLCOMS is well suited to maintaining sharp temperature and salinity gradients that are abundant in shelf seas. The High Resolution Continental Shelf (HRCS) setup with 32 vertical σ-coordinate layers and approximately 1.8 km horizontal resolution is used for all model simulations. This has a finer horizontal resolution than the MRCS setup (approximately 7 km horizontal resolution, 18 vertical layers) used in a previous study (Blackford et al., 2008), and is known to have some improvements, particularly in the estimation of currents near fronts and the flow entering the Skagerrak (Holt and Proctor, 2008). POLCOMS is coupled to GOTM (Umlauf and Burchard, 2003) to calculate the turbulent kinetic energy with the k–ε turbulence closure scheme, which is then used to derive eddy viscosity and diffusivity using the stability relations of Canuto et al. (2001).

The CO_2 or carbonate system is simulated using an iterative speciation model based on HALTAFALL (Ingri et al., 1967), as applied in Blackford and Gilbert (2007), Blackford et al. (2008) and Artioli et al. (2012) with dissolved inorganic carbon (DIC) and total alkalinity (TA) as master variables. Coupled with information of the primary physical properties (temperature, salinity and pressure) delivered

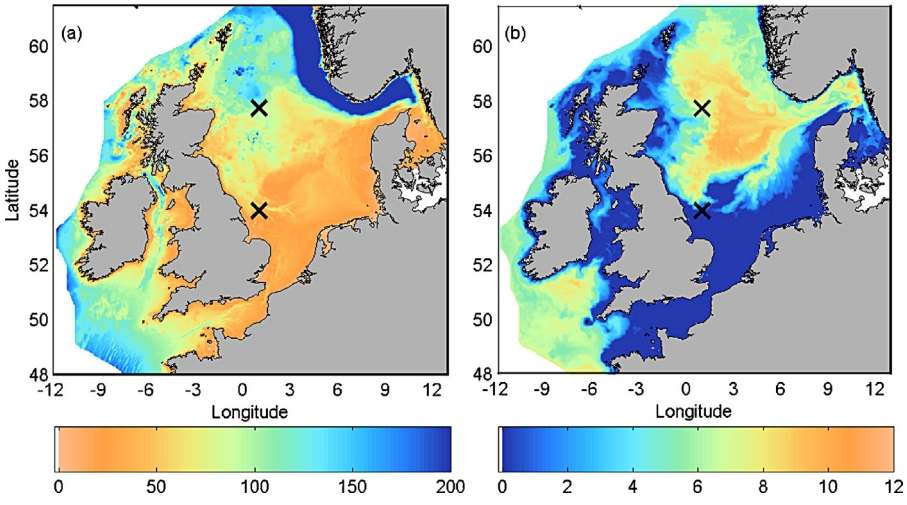

Fig. 1. (a) Bathymetry (m) in the POLCOMS HRCS model domain. The colour axis is capped at 200 m to show greater detail in the region of interest. (b) Surface temperature minus bottom temperature (°C) on 1st September 1999 according to POLCOMS output. CO_2 leakage sites are denoted by black crosses.

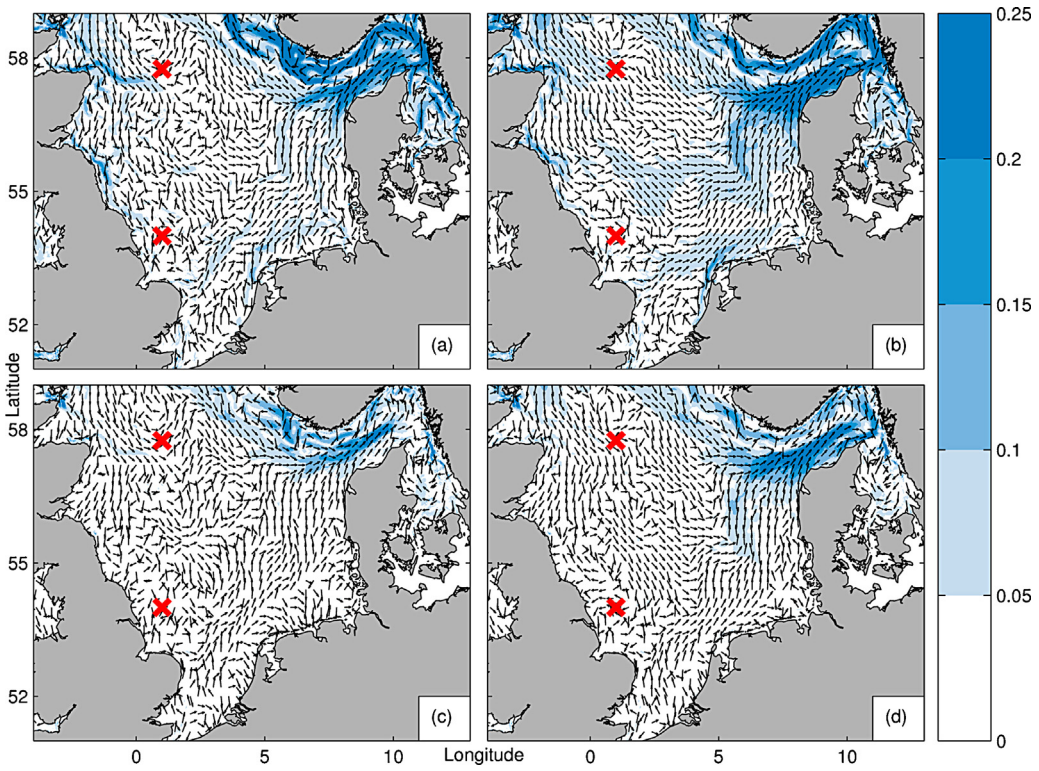

Fig. 2. Mean velocity (m/s) in the North Sea according to POLCOMS output. Black arrows (shown every 12th grid cell) depict direction, the colour corresponds to the magnitude. (a) Summer surface; (b) winter surface; (c) summer bottom; (d) winter bottom. Summer plots give the average velocity between June and August 1999. Winter plots give the average between December 1999 and February 2000. Surface plots show the average between the surface and 10 m depth. Bottom plots show the average velocity between 40 m depth and the seabed (or bottom grid cell where depths are shallower than 40 m). The colour axis is capped at 0.25 m/s to show greater detail in the region of interest.

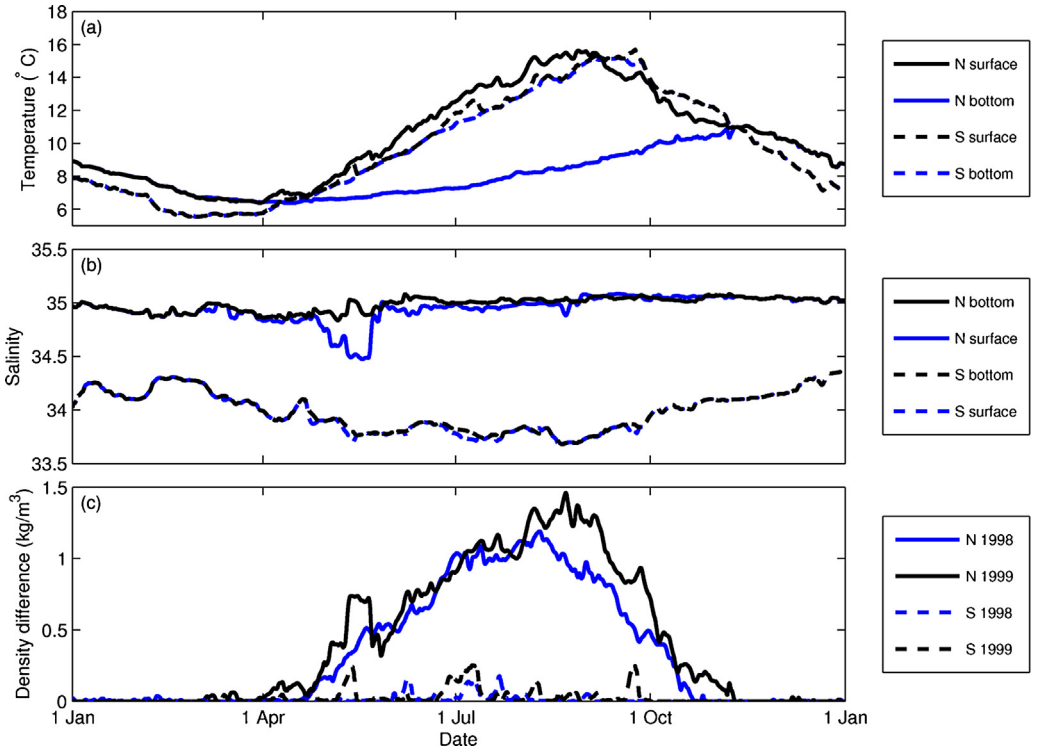

Fig. 3. Time series data at the two CO_2 release sites (N, north site; S, south site) from POLCOMS model output. (a) Surface and bottom temperature in 1999. (b) Surface and bottom salinity in 1999. (c) Comparison of stratification (bottom density minus surface density) in 1998 and 1999.

by POLCOMS the model derives the carbonate system parameters of interest, in particular pH and the saturation states of calcite (Ω_{cal}) and aragonite (Ω_{arg}) which are used here as metrics of impact.

For the purpose of this study DIC was divided into two components, representing the background DIC (DIC_B) and the additional DIC as a result of a geological carbon storage leak (DIC_L). For clarity the sum of these two components will henceforth be referred to as the total DIC (DIC_T),

$$DIC_T = DIC_B + DIC_L.$$

Both DIC_B and DIC_L were treated as three dimensional scalar fields, advected and diffused within the hydrodynamic model. By separating DIC_T into two components and omitting the use of a coupled ecosystem model (such as ERSEM) the complexity of the model is reduced significantly, however this approach means that any nonlinear biological feedback caused by the injection of additional DIC_L into the ecosystem is neglected. As the North Sea marine ecosystem is not carbon limited, these nonlinear feedbacks are believed to be minimal.

Background DIC_B is initialised to zero and relaxed to monthly mean DIC data generated by the coupled hydrodynamic-ecosystem model POLCOMS-ERSEM (AMM setup) (Wakelin et al., 2012), interpolated in space onto the HRCS grid and linearly in time to each model time step, with a relaxation period of one week. This provides a reasonable proxy for the normal seasonal and spatial dynamics of DIC_B.

The small-scale dynamics of CO_2 bubble plumes are highly complex and research into the subject is ongoing. In a recent small-scale two-fluid modelling investigation into the impact of CO_2 injection in the North Sea, Dewar et al. (2013) found that CO_2 bubbles have a fast rise velocity but also a quick dissolution rate, and whilst plume height was influenced by a number of factors including tidal flow, temperature and leakage rate, all injected CO_2 dissolved within a few metres. Furthermore in a controlled CO_2 leakage experiment in a coastal loch, the QICS research consortium (QICS, 2012) observed that the majority of CO_2 bubbles dissolved in the first 10 m of upward flow. Consequently, all DIC_L source terms are injected directly into to the bottom layer of a single grid cell at the two leakage sites, with various leakage scenarios as described in Section 2.3. The air–sea flux of leakage DIC_L is calculated using the scheme of Nightingale et al. (2000) by subtracting the background CO_2 flux (using pCO_2 derived from DIC_B) from the total CO_2 flux (using pCO_2 derived from DIC_T), as air–sea fluxes of DIC_B are already accounted for in the background data.

Haugan and Drange (1992) first brought attention to the effect of dissolved CO_2 on seawater density and highlighted the fact that in extreme cases injections of dissolved CO_2 could result in sufficiently large density modifications to drive a density current. More recently there have been numerous attempts to determine the equation of state for a CO_2 solution (Ohsumi et al., 1992; Song et al., 2002; Duan and Zhang, 2006). For this research the following density modification of Song et al. (2002) is used,

$$\Delta\rho = 275.47\chi,$$

where χ represents the mass fraction of CO_2 in the solution

$$\chi = \frac{\rho_{CO_2}}{\rho_s + \rho_{CO_2}}$$

Here ρ_{CO_2} is taken to be the density of the freshly dissolved CO_2 due to the simulated leak and ρ_s represents the density of seawater in absence of the added CO_2. In the model, CO_2 is a diagnostic variable that is derived from prognostic variables (DIC, TA, etc.), so the concentration of CO_2 attributed to the leakage DIC_L is assumed to be equal to the following term

$$[\Delta CO_2] = [CO_2]\big|_{DIC_T} - CO_2\big|_{DIC_B}\ \text{mmol/m}^3.$$

In extremely large CO_2 concentrations the density effect may be significant ($\Delta\rho \approx 0.1\ \text{kg/m}^3$ at CO_2 concentrations of the order of $10\ \text{mol/m}^3$), however changes to density are likely to be minimal outside the vicinity of the source at the leakage rates considered in this study.

TA is considered to be the sum of a diagnostic component and a prognostic component following an improved approach for calculating TA in shelf seas (Artioli et al., 2012).

$$TA = TA_{dia} + TA_{pro}.$$

TA_{dia} is calculated from the linear relation between TA and salinity S in the Atlantic Ocean (Millero et al., 1998),

$$TA_{dia} = 51.24S + 520.1,$$

whilst TA_{pro} is treated as a conservative scalar, advected and diffused in POLCOMS with source terms at the riverine grid cells (representing the contribution of riverine TA). For further details of this approach and for the derivation of riverine TA concentrations see Artioli et al. (2012), although note that the sink terms representing the biochemical contribution to TA_{pro} are not included in the present study due to the lack of a coupled ecosystem model.

The carbonate model uses the OCMIP recommendations for the set of constants, i.e. using the Weiss (1974) formulation of Henry's constant for CO_2, the dissociation constants for carbonic acid defined by Millero (1995) using the refit of Mehrbach et al. (1973), and the borate dissociation constant from Millero (1995) using data from Dickson (1990).

2.3. Leakage scenarios

A series of short-term and long-term leakage scenarios were devised to investigate the range of potential impacts of geological CO_2 release in the North Sea. During the short-term model runs CO_2 is released at the two leakage sites at a constant rate of 5000 t CO_2 per day for one day before being "switched off". The recovery of the carbonate system is monitored for the remainder of the month. This scenario represents a quick release of CO_2 that is quickly identified and promptly repaired, such as a pipeline failure. The release rate used here is approximately twice the CO_2 pipeline capacity at the currently operating Sleipner plant (Statoil, 2013).

During the long-term simulations, CO_2 is injected continuously for a full year, representing a failure of the carbon sequestration reservoir, such as a leak through a geological fault that may be extremely difficult to repair. The carbonate system is monitored throughout the duration of the CO_2 leak and for the initial three months of the recovery period. IEAGHG (2009) reported a range of plausible long-term CO_2 leakage rates extending from 1 to 50,000 t CO_2 per day. Scale analysis shows that leakages closer to the lower end of this range will scarcely be detectable at the resolution of the model used within the present study, and regional hydrodynamic models with finer resolution would be better suited to investigate the impacts of such leakages over small scales. Therefore the decision was taken to conduct the long-term simulations with constant leakage rates of 1000 and 10,000 t CO_2 per day.

In order to investigate the seasonal and inter-annual variability of the impacts of CO_2 leakages, each short-term experiment is repeated with a release in January, April, July and October of 1998 and 1999, and the long-term simulations are repeated with a release beginning in January and July of 1998 and 1999. Each simulation begins on 1st January 1995, providing a minimum of a 3-year spin-up period to ensure that salinity, temperature, DIC_B and

Table 1
Details of the duration and size of the CO_2 source term for each model run. Model spin-up begins on 1st Jan 1995 for every run.

Run	Leak start	Leak duration (days)	Leak size (t CO_2 day)
Short-term leakage scenarios			
ST1	1st January 1998	1	5000
ST2	1st April 1998	1	5000
ST3	1st July 1998	1	5,000
ST4	1st October 1998	1	5000
ST5	1st January 1999	1	5000
ST6	1st April 1999	1	5000
ST7	1st July 1999	1	5000
ST8	1st October 1999	1	5000
Long-term leakage scenarios			
LT1	1st January 1998	365	10,000
LT2	1st July 1998	365	10,000
LT3	1st January 1999	365	10,000
LT4	1st July 1999	365	10,000
LT5	1st January 1998	365	1000
LT6	1st July 1998	365	1000
LT7	1st January 1999	365	1000
LT8	1st July 1999	365	1000

TA_{pro} have reached appropriate values and stabilised prior to the introduction of leakage DIC_L. Years 1998 and 1999 were selected to give two consecutive years with contrasting mean North Atlantic Oscillation (NAO) indices (NOAA, 2013), as the NAO is believed to influence the wind driven circulation and mixing in the North Sea.

The seasonal stratification is slightly stronger at the north site during 1999 than 1998 (Fig. 3c). Although the south site experiences no prolonged periods of enduring stratification in either year, the temporary periods of stratification are both more frequent and stronger during 1999. Full details of each model run are given in Table 1.

3. Results

We present the majority of the results by referencing the change in pH caused by the additional CO_2. Normal marine pH is in the region of 8.1 and varies naturally by around ±0.2 units in shelf systems, although larger variations can be associated with coastal features (Blackford and Gilbert, 2007). It is established that marine biota and biogeochemical processes are sensitive to pH, although this sensitivity is complex. In order to give context to the results presented, long-term reductions in pH approaching or exceeding 1.0 unit can be considered as significantly harmful, reductions of the order of 0.2–0.5 as potentially harmful whilst reductions of <0.1 unit are unlikely to have an impact (Widdicombe et al., 2013). Short-term (hours to a few days) reductions in pH will be much less deleterious to marine biota. In terms of monitoring for leakage, current instrumentation can resolve pH changes of 0.01 unit or greater (Rerolle et al., 2013). The limiting factor in monitoring for leakage is therefore distinguishing leakage signals from natural variability.

3.1. Short-term leakage scenarios

Significant changes in the marine carbonate system are observed in each of the short-term leakage scenarios, however any perturbations are minimal outside the vicinity of the source. Across all eight simulations the largest recorded reductions to seawater pH are 1.92 and 1.22 pH units at the north and south site respectively, both occurring during the ST4 scenario, yet reductions are typically weaker than 0.1 pH units beyond 10 km from the release sites (see Table 2, Fig. 4). Significant perturbations to pH are generally restricted to the bottom layer, even at the vertically mixed south site, and reductions to surface pH are typically weaker than 0.1 pH units (Figs. 5 and 6). It is evident that any CO_2 plumes arising from leakages of this magnitude are highly localised in the context of the North Sea.

The results show that calcite is only briefly undersaturated at both sites, and this is spatially confined to the release sites and adjacent grid cells. Undersaturation of aragonite extends only slightly further at the north site, reaching approximately 4 km from the CO_2 source. Both minerals return to supersaturated levels within a single day after the end of the release period in all simulations and at both sites. It is apparent that the 1.8 km grid resolution is not sufficiently fine to properly resolve the small undersaturated region for CO_2 leakages of this magnitude.

The carbonate system at the leakage sites quickly returns to background values after the end of the CO_2 release period. This is primarily due to advection of CO_2 away from the leakage sites and tidal mixing rather than outgasing of CO_2 at the sea surface, and a rapid recovery is also observed at the north site during the summer months when outgasing is negligible. During the recovery period the greatest reduction in seawater pH is generally not found at the release sites but at nearby locations, as the CO_2 plumes are gradually advected further away from their source point. Across all leakage scenarios the reductions to pH are weaker than 0.1 pH units within 5 days and below 0.05 pH units within 8 days within the northern CO_2 plume. In the southern CO_2 plume all reductions are weaker than 0.1 pH units within 3 days and below 0.05 pH units within 7 days. By day 30 the greatest reductions to seawater pH are less than 0.014 pH units at both sites. The concentration of CO_2 at the release sites is observed to oscillate periodically during some simulations due to semi-diurnal tidal advection.

Table 3 displays the proportion of the injected CO_2 that had escaped into the atmosphere 30 days after the start of the CO_2 release period. Across all eight simulations an average of 25.0% outgases at the south site by the end of the 30 days, meanwhile only 6.2% typically escapes the water column at the north site over the same period. There are significant variations between release scenarios at the north site as there is minimal outgasing during the summer releases due to the sharp thermocline. By contrast, the pathway and strength of the acidified plume at the south site is more consistent between simulations. There is also considerable inter-annual variability at the north site, as the proportion of

Table 2
Greatest horizontal distance (rounded to nearest km) between the release sites and three critical ΔpH contours for each short-term release scenario. Values represent the greatest distance over the whole simulation. Note that the horizontal grid resolution is approximately 1.8 km, therefore low values should be treated with caution as these contours will be highly dependent upon the grid resolution.

Station	ΔpH	ST1	ST2	ST3	ST4	ST5	ST6	ST7	ST8
North site	0.1	6	6	17	8	8	8	8	8
	0.05	8	8	42	9	11	11	13	28
	0.01	37	102	102	61	61	61	92	93
South site	0.1	4	4	6	9	9	9	9	9
	0.05	35	35	35	20	23	23	23	23
	0.01	108	108	108	104	116	116	116	116

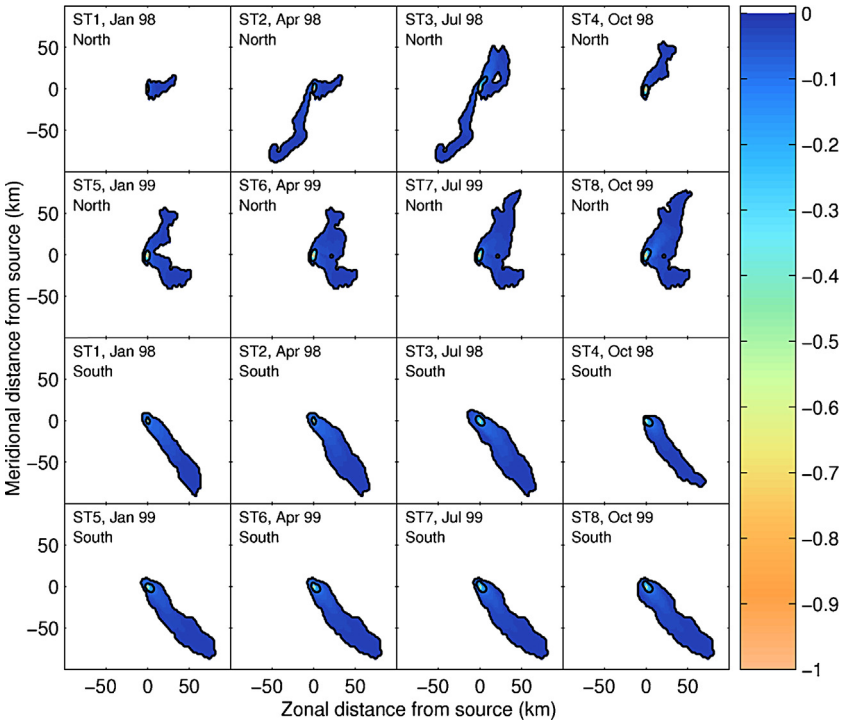

Fig. 4. Maximum perturbation to pH at the seabed over each short-term simulation. Each figure shows a 200 km by 200 km grid surrounding the release site. The −0.1 and −0.01 pH unit contours are highlighted and changes of less than 0.01 pH units have been masked.

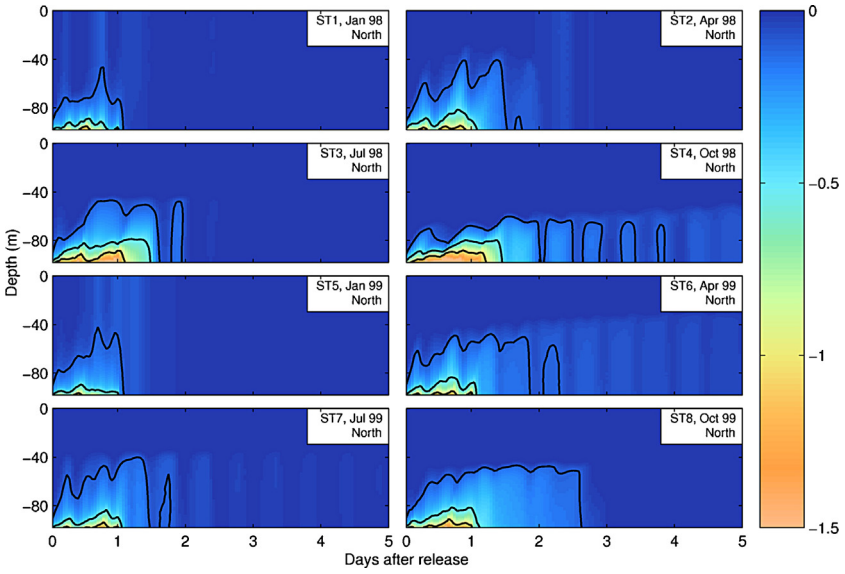

Fig. 5. Time series of the perturbation to pH throughout the water column at the north site during the first 5 days of the simulation for the short-term leakage scenarios. Contours of −1.0, −0.5 and −0.1 pH units have been highlighted.

escaped CO_2 in the April and October 1998 release scenarios (ST2 and ST4) is considerably greater than the corresponding releases in 1999 (ST6 and ST8). This can be explained by the fact that stratification develops earlier and breaks down later during the 1999 run.

3.2. Long-term leakage scenarios

The long-term scenarios with release rates of 10,000 t CO_2 per day (LT1–LT4) result in extensive plumes of highly acidified water that extend from the source locations (Fig. 7a and b). At the north

Table 3
Percentage of additional CO_2 released into atmosphere 30 days after the start of the CO_2 release, short-term leakage scenarios ST1 to ST8.

	ST1	ST2	ST3	ST4	ST5	ST6	ST7	ST8
North site	11.5%	12.9%	<0.01%	6.0%	14.4%	3.8%	<0.01%	0.8%
South site	31.6%	22.3%	15.2%	33.4%	39.9%	24.3%	14.2%	18.9%

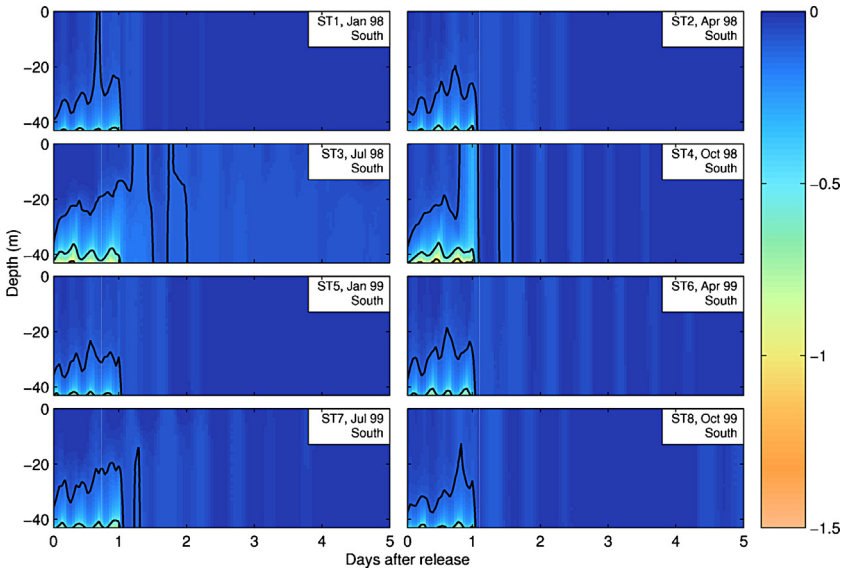

Fig. 6. Time series of the perturbation to in pH throughout the water column at the south site during the first 5 days of the simulation for the short-term leakage scenarios. Contours of 1.0, 0.5 and 0.1 pH units have been highlighted.

site most of the CO_2 is carried initially northward then eastward by the mean circulation, broadly reflecting the Dooley Current, and gradually spreads laterally to the north and south. However, a considerable proportion is also advected south of the release station. The pathway of CO_2 released at the south site appears to be much more persistent, initially flowing in a slow and narrow south-eastward pathway adjacent to the English coastline, then rapidly advancing north-eastward towards the Skagerrak in a much weaker concentration. The greatest reductions to pH are 2.67 and 2.32 pH units at the north and south site respectively, whilst acidification by 1.0 pH units could be found as far as 39 km from the north site, and 24 km from the south site. These scenarios result in large regions where calcite is undersaturated, extending as far as 62 km from the north site, and 70 km from the south site. Aragonite was undersaturated as far as 126 and 118 km from the north and south site respectively.

Leakages of 1000 t CO_2 per day (LT5–LT8) result in plumes of acidified water that follow identical pathways to those described for the larger release rate; however reductions to seawater pH are generally an order of magnitude weaker throughout most of the domain (Fig. 7c and d). The largest reductions to seawater pH across these four scenarios are 1.19 and 0.98 pH units at the north site and south site respectively. These scenarios cause no undersaturation of calcite outside the CO_2 source grid cells, and only minimal

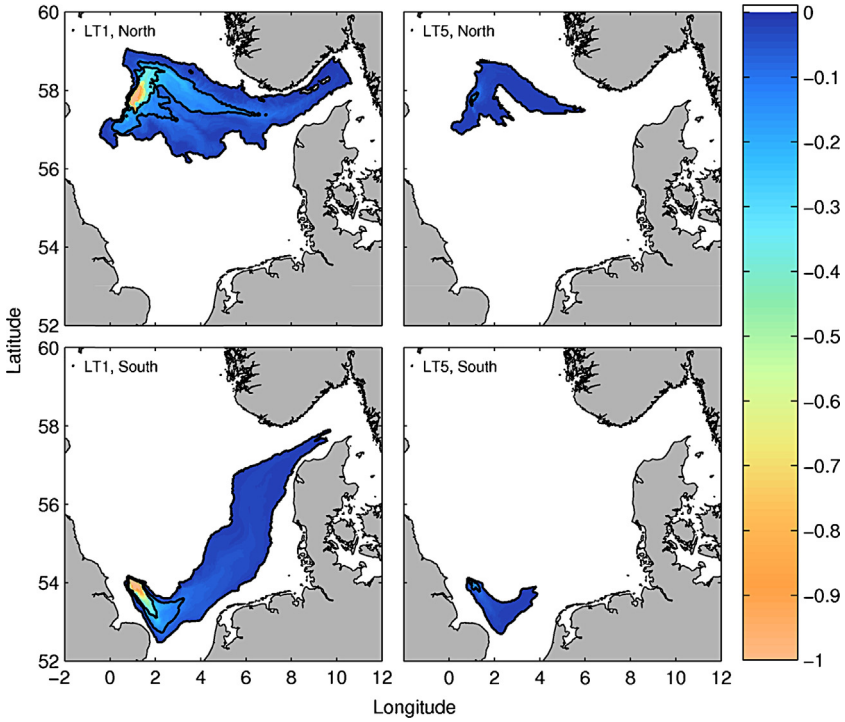

Fig. 7. Maximum perturbation pH at the seabed over the long-term simulations LT1 (10,000 t CO_2/day, January 1998 start) and LT5 (1000 t CO_2/day, January 1998 start), with the −0.25, −0.1 and −0.01 pH unit contours highlighted. The colour bar has been capped at 1 pH units. Changes of less than 0.01 pH units have been masked.

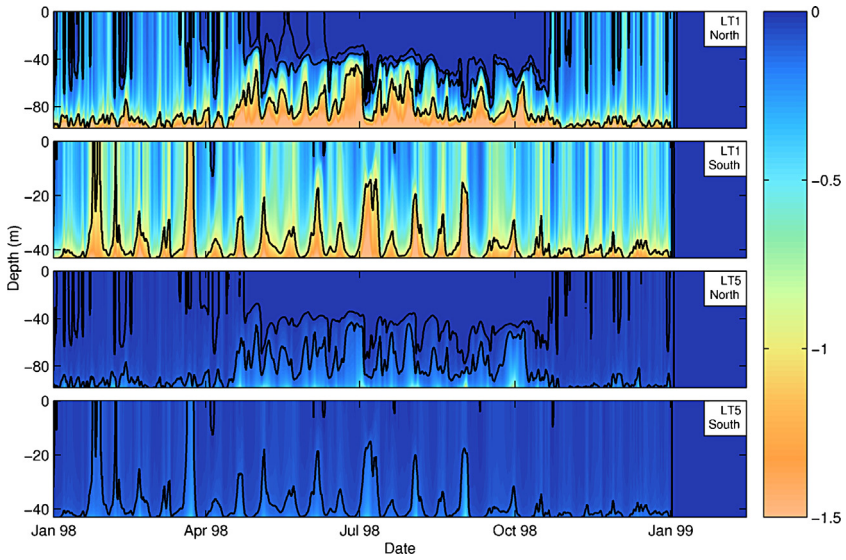

Fig. 8. Time series of perturbation to pH over the LT1 scenario (10,000 t CO_2/day, January 1998 start) and LT5 scenario (1000 t CO_2/day, January 1998 start) at the north and south sites. Hourly output has been smoothed with a moving average filter (span of 25 h) to reduce diurnal variability. The 1.0, 0.1 and 0.01 pH contours have been highlighted.

undersaturation of aragonite, extending no further than 6 km from either site.

The carbonate system at both release sites returns to natural values almost instantly after the end of the CO_2 release period (Fig. 8); however this is misleading as once again the rapid recovery is due to advection away from the source rather than outgasing, and acidified water continues to linger in the North Sea for some time afterwards (Fig. 9). Fig. 8 demonstrates the influence of stratification upon the fate of released CO_2 as the impact on bottom pH is intensified at the north site during the summer months, whilst the influence on surface pH is negligible. Another feature that is particularly apparent at the south site is a regular oscillation in pH in synchronisation with the spring-neap cycle. Strong tidal advection during spring tides mean the CO_2 is injected into a larger volume of water in weaker concentrations, and the energetic turbulence ensures the CO_2 is well mixed. In contrast neap tides allow CO_2 to accumulate at the release site in large concentrations, causing greater reductions to seawater pH (Table 4).

On average 40.2% of the CO_2 added at the north site outgases by the end of the ninety days, whereas the average figure is 86.4% at the south site (Table 5). There is little variability in the proportion of outgased CO_2 between different leakage scenarios because long release durations ensure that each simulation contains similar periods when the water column is stratified and vertically mixed (Fig. 10).

There is significant seasonal variability in the rate of CO_2 outgasing within each individual simulation, and this is particularly evident at the north site (Fig. 11). The air–sea flux of CO_2 is generally slightly greater during 1998 than 1999 at the north site due to the shorter duration of stratification, whereas there is no

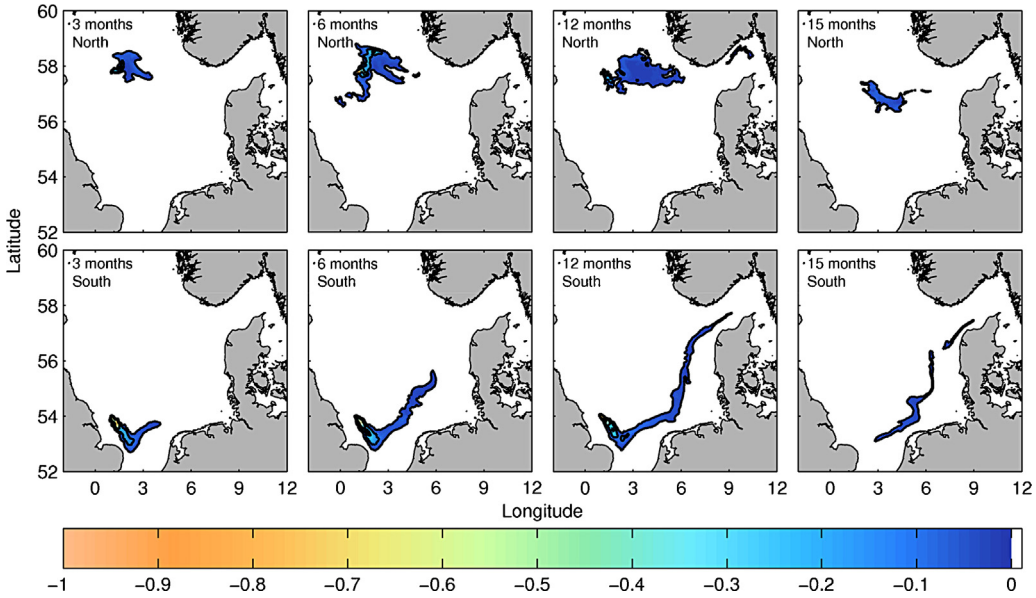

Fig. 9. Snapshots of the perturbation to pH at the seabed during the LT1 scenario at both release sites. The −0.25, −0.1 and −0.01 pH unit contours are highlighted and perturbations of less than 0.01 pH units have been masked. The colour bar has been capped at 1 pH units. Labels (3, 6, 9, 15 months) indicate the length of time elapsed since the start of the initial CO_2 injection. The 15-month snapshot shows the pH perturbation after 3 months of recovery.

Table 4
Greatest horizontal distance (rounded to nearest km) between the release sites and five critical ΔpH contours for each long-term release scenario. Values represent the greatest distance over the whole simulation. A value of 0.0 indicates that such perturbations are found at the release site only. A 'X' indicates that no such perturbations are found anywhere.

	ΔpH	LT1	LT2	LT3	LT4	LT5	LT6	LT7	LT8
North site	1.0	39	21	34	30	0	X	X	0
	0.5	61	49	54	54	0	0	0	0
	0.25	117	103	108	141	6	4	2	2
	0.1	354	306	378	347	26	16	18	16
	0.01	570	575	580	58	299	334	303	322
South site	1.0	23	22	24	24	X	X	X	X
	0.5	62	61	62	57	X	0	0	0
	0.25	122	100	99	108	2	2	2	2
	0.1	166	156	165	160	35	22	33	33
	0.01	693	670	461	437	193	186	196	18

Table 5
Percentage of additional CO_2 released into atmosphere 90 days after the end of the CO_2 release (455 days after the initial CO_2 injection), long-term leakage scenarios LT1–LT8.

	LT1	LT2	LT3	LT4	LT5	LT6	LT7	LT8
North site	46.0%	38.8%	40.2%	38.0%	44.7%	37.2%	39.1%	37.2%
South site	90.7%	84.5%	92.9%	85.6%	87.3%	79.5%	90.3%	80.7%

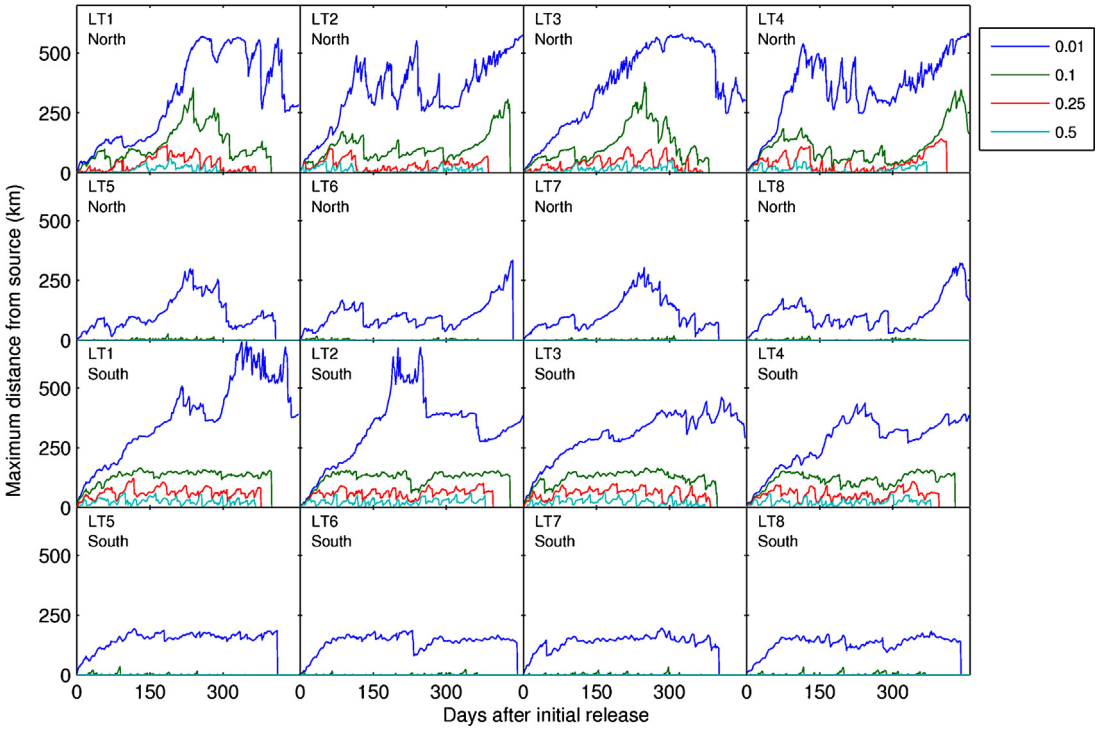

Fig. 10. Greatest distance of four critical pH perturbation contours from the source over time for long-term leakage simulations.

significant inter-annual variability in outgasing at the south site. At the south site a greater proportion of CO_2 escapes the water column during the first four leakage scenarios with the larger CO_2 source term, this can be explained by the buffering of CO_2 in seawater. This variability according to the magnitude of the CO_2 source term is less pronounced at the north site as the large depths and strong summer stratification mean that the added CO_2 is well mixed and somewhat diluted before it reaches the surface layer.

4. Discussion

Leakage scenarios ranging from pipeline leakages (with a release rate of 1000 t CO_2 per day) to the complete failure of a carbon sequestration facility (with a release rate of 10,000 t CO_2 per day) were simulated for a modelling investigation into the effects of large geological CO_2 leakages on the North Sea carbonate system. Short-term leakages of 5000 t CO_2 over a single day result in significant acidification at the release sites, reducing pH by as much as 1.92 pH units. Perturbations of 0.1 pH units and greater were generally confined to a restricted region at any point in time (in the context of the size of the study region), typically smaller than 10 km in diameter; however strong mean circulation and semi-diurnal tidal advection meant that such reductions in pH were found as far as 17 km from the source point. By contrast long-term leakages of 1000 t CO_2 per day for a year only reduced the pH by a maximum of 1.19 pH units at the release site, and local perturbations were considerably weaker than those in the short-term leakage scenarios. This highlights the fact that added CO_2 is rapidly flushed away from the source, and a single burst of CO_2 at a high rate will result in greater perturbations to the carbonate system over

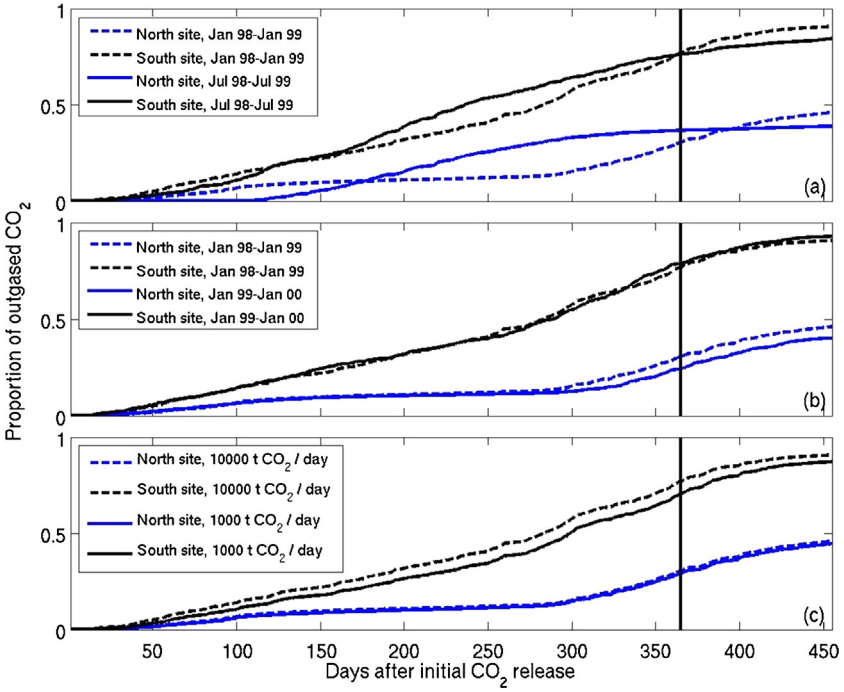

Fig. 11. Comparison of CO_2 outgasing rates. (a) Seasonal variability (LT1 and LT2). (b) Inter-annual variability (LT1 and LT 3). (c) Variability due to CO_2 leakage rate (LT1 and LT5).

short distances than a slower sustained release. Over greater spatial scales the long-term leakages had a much more significant impact upon the carbonate system than the short-term releases, causing reductions of 0.1 pH units as far as 35 km from the release point, and reductions of 0.01 pH units over several hundred kilometres. Finally the long-term leakages of 10,000 t CO_2 per day for a full year caused widespread acidification across the North Sea, reducing pH by up to 2.67 pH units at the release sites and causing reductions of 0.25 pH units as far as 141 km away from the source. It should be emphasized though that this is a very unlikely scenario.

Any predicted acidification should be considered in the context of natural variability of pH in the North Sea, which can exceed 1.0 pH units in coastal regions of freshwater influence, although further offshore in regions of low biological activity annual variability is typically around 0.1–0.2 pH units (Blackford and Gilbert, 2007). Furthermore, the North Sea is expected to acidify by an average of 0.2 pH units compared to pre-industrial levels by the year 2050 due to anthropogenic CO_2 emissions, and by an additional 0.13–0.28 pH units by 2100 (Blackford and Gilbert, 2007). Therefore throughout most of the North Sea, continued unmitigated CO_2 emissions will result in greater, ubiquitous and more long-lived acidification over the next few decades than even the worst case scenario investigated here. It should be highlighted however that any acidification due to CO_2 leakages would be in addition to natural variability, and the rate of acidification would be considerably faster than the long-term trend associated with rising atmospheric CO_2.

It is difficult to determine precisely how the carbonate system would react to CO_2 leakages under the environmental conditions of the future, when CCS is conducted on a larger scale. It is anticipated that atmospheric pCO_2 will continue to increase along with surface temperatures, causing seawater pH to decrease, shifting the partitioning of DIC in favour of CO_2. At the same time the buffering capacity of seawater will decrease, implying that for a given increase in DIC the decrease in pH will be greater. Although any increase in surface temperatures will lead to a decrease in the solubility of CO_2 in seawater, potentially increasing the rate of outgasing further, greater thermal stratification may tend to isolate sea floor leakages from the surface, decreasing outgassing. This is somewhat speculative due to the complex nature of the carbonate system, and other factors such as potential changes to wind intensity could complicate this matter further. There is clearly a need for further research to focus upon the response of the carbonate system to CO_2 leakages under projected future climate conditions.

Whilst the results presented here give considerable insight into the impact of large CO_2 additions upon the physical and chemical environment, the impact of acidification upon the marine ecosystem would ultimately depend upon the tolerance of resident biota to perturbations to pH and the saturation states of calcite and aragonite, and a detailed assessment of this is beyond the scope of this article. With the exception of the worst case scenarios, LT1–LT4, the simulations investigated here generally only caused significant perturbations to the carbonate system over spatial scales of the order of 50 km, and whilst release rates of 1000 t CO_2 per day caused reductions of 0.01 pH units over hundreds of kilometres from the source, in reality such small changes would be indistinguishable from background variability, and they would have no deleterious consequences for marine fauna and flora. It would therefore appear sensible for future modelling studies to utilise local hydrodynamic models with finer horizontal resolution to investigate the impacts of smaller CO_2 leakages over more confined spatial scales.

The influence of stratification upon the fate of a CO_2 plume was evident in every set of release scenarios considered here. Strong seasonal thermoclines are able to inhibit the exchange of CO_2 between surface and bottom waters, and ultimately prevent outgasing of CO_2 into the atmosphere. Overall the carbonate system at the south site would appear to be considerably less sensitive to CO_2 additions than the north site, primarily because the shallow depths and generally well mixed vertical profile mean CO_2 can readily escape to the atmosphere, and strong tidal currents ensure that CO_2 is well mixed within the water column. Although seasonal variability to the air–sea flux was significant at both sites, on average the CO_2 injected at the south site reached the atmosphere twice as fast as the corresponding CO_2 at the north site. Furthermore Thomas et al. (2004) reported that on average the southern

North Sea is super-saturated with CO_2 whereas the northern North Sea is generally undersaturated, and this is particularly clear during the summer. Although pCO_2 is not replicated particularly well by the POLCOMS-ERSEM–HALTAFALL model (Artioli et al., 2012), in reality this pattern would reinforce the spatial variability highlighted by this study, as added CO_2 would leave the water column faster in an outgasing regime. Although there are many additional factors to consider when assessing potential carbon sequestration sites, including the biodiversity of the environment, the feasibility and cost of installation and maintenance, and the likelihood of sequestered CO_2 entering the water column, this investigation would suggest that if all other factors are equal, the physical marine environment of the shallow, well-mixed southern North Sea is less sensitive to CO_2 inputs than the deeper, seasonally stratified northern North Sea.

The results of this investigation are broadly in good agreement with Blackford et al. (2008), however there are some notable differences between the two studies due to the model improvements, particularly in the local pH perturbations. For example, in their high long-term seepage scenario (3.02×10^5 t CO_2 over a year), Blackford et al. (2008) found that that perturbations to pH reached a maximum of 0.12 pH units, whereas the LT5–LT8 scenarios in the present study (3.65×10^5 t CO_2 over a year) show perturbations exceeding 1 pH unit at the seabed. Similarly the previous investigation reports that low short-term leaks (1.49×10^4 t CO_2 over a single day) result in reductions of up to 0.2 pH units, whereas short-term scenarios ST1–ST8 (5×10^3 t CO_2 over a single day) in the current investigation show perturbations reaching 1.92 pH units, despite the much smaller release. This can be explained by the improvements in model resolution, and the fact that CO_2 is injected only into the bottom grid cell in this study. The volume of seawater receiving the CO_2 source term is approximately two orders of magnitude smaller than the volume in the previous investigation, and as a result CO_2 concentrations are much greater, and local pH reductions are far more significant. This supports the assertion of the previous study that it is likely that such events would have a catastrophic impact on the environment on a localised scale (<1 km).

This study confirms previous work that suggests that only the largest conceivable leakage events would have significant environmental impact over large spatial scales in the context of the functionality of the North Sea. In the largest release scenarios investigated here, reductions of 0.1 pH units were detected 10 km downstream of the source within a couple of days of the start of the CO_2 release, and were found 50 km downstream within a month. Such events should be readily detectable and conversely, lack of detection of such events, given good monitoring practice, could be taken as conclusive proof that such leakages were not occurring.

Acknowledgements

This work was undertaken by the QICS project funded by the RCUK/NERC (NE/H013849/1 and NE/H013962/1). Additional funding was also provided by the lead author's RCUK/NERC studentship (NE/I528042/1) and from the Scottish Government. We also thank the anonymous reviewers for their helpful comments.

References

Arakawa, A., Lamb, V.R., 1977. Computational design of the basic dynamical processes of the UCLA generic circulation model. Methods Comput. Phys. 17, 173–265.

Artioli, Y., Blackford, J.C., Butenschon, M., Holt, J.T., Wakelin, S.L., Thomas, H., Borges, A.V., Allen, J.I., 2012. The carbonate system in the North Sea: sensitivity and model validation. J. Mar. Syst. 102, 1–13.

Blackford, J.C., Gilbert, F.J., 2007. pH variability and CO_2 induced acidification in the North Sea. J. Mar. Syst. 64 (1–4), 229–241.

Blackford, J.C., Jones, N., Proctor, R., Holt, J., 2008. Regional scale impacts of distinct CO_2 additions in the North Sea. Mar. Pollut. Bull. 56 (8), 1461–1468.

Canuto, V.M., Howard, A., Cheng, Y., Dubovikov, M.S., 2001. Ocean turbulence. Part I: one-point closure model – momentum and heat vertical diffusivities. J. Phys. Oceanogr. 31 (6), 1413–1426.

Colella, P., Woodward, P.R., 1984. The piecewise parabolic method (PPM) for gas-dynamical simulations. J. Comput. Phys. 54 (1), 174–201.

Dewar, M., Wei, W., McNeil, D., Nishio, M., Chen, B., 2013. Simulation of the near field physiochemical impact of CO_2 leakage into shallow water in the North Sea. GHGT-11. Energy Procedia 37.

Dickson, A.G., 1990. Thermodynamics of the dissociation of boric-acid in synthetic seawater from 273.15-K to 318.15-K. Deep-Sea Res. A: Oceanogr. Res. Pap. 37 (5), 755–766.

Duan, Z.H., Zhang, Z.G., 2006. Equation of state of the H_2O, CO_2, and H_2O–CO_2 systems up to 10 GPa and 2573.15 K: molecular dynamics simulations with ab initio potential surface. Geochim. Cosmochim. Acta 70 (9), 2311–2324.

Haugan, P.M., Drange, H., 1992. Sequestration of CO_2 in the deep ocean by shallow injection. Nature 357 (6376), 318–320.

Holt, J.T., James, I.D., 2001. An s coordinate density evolving model of the northwest European continental shelf – 1, model description and density structure. J. Geophys. Res.: Oceans 106 (C7), 14015–14034.

Holt, J., Proctor, R., 2008. The seasonal circulation and volume transport on the northwest European continental shelf: a fine-resolution model study. J. Geophys. Res.: Oceans 113 (C6).

IEAGHG, I. G. G. R. D. P., 2009. Assessment of Sub-sea Ecosystem Impacts. IEA Greenhouse Gas R&D, Cheltenham, UK.

Ingri, N., Kakolowi, W., Sillen, L.G., Warnqvis, B., 1967. High-speed computers as a supplement to graphical method, V. Haltafall a general program for calculating composition of equilibrium mixtures. Talanta 14 (11), 1261.

James, I.D., 1996. Advection schemes for shelf sea models. J. Mar. Syst. 8 (3–4), 237–254.

Mehrbach, C., Culberso, Ch, Hawley, J.E., Pytkowic, R.M., 1973. Measurement of apparent dissociation-constants of carbonic-acid in seawater at atmospheric-pressure. Limnol. Oceanogr. 18 (6), 897–907.

Millero, F.J., 1995. Thermodynamics of the carbon-dioxide system in the oceans. Geochim. Cosmochim. Acta 59 (4), 661–677.

Millero, F.J., Lee, K., Roche, M., 1998. Distribution of alkalinity in the surface waters of the major oceans. Mar. Chem. 60 (1–2), 111–130.

National Research Council (U.S.), Committee on the Safety of Marine Pipelines, 1994. Improving the Safety of Marine Pipelines. National Academy Press, Washington, D.C.

Nightingale, P.D., Malin, G., Law, C.S., Watson, A.J., Liss, P.S., Liddicoat, M.I., Boutin, J., Upstill-Goddard, R.C., 2000. In situ evaluation of air-sea gas exchange parameterizations using novel conservative and volatile tracers. Glob. Biogeochem. Cycles 14 (1), 373–387.

NOAA, N.W.S., 2013. Climate Prediction Center – Teleconnections: North Atlantic Oscillation, Available from: http://www.cpc.ncep.noaa.gov/products/precip/CWlink/pna/nao.shtml

Ohsumi, T., Nakashiki, N., Shitashima, K., Hirama, K., 1992. Density change of water due to dissolution of carbon-dioxide and near-field behavior of CO_2 from a source on deep-sea floor. Energy Convers. Manag. 33 (5–8), 685–690.

QICS, 2012. Quantifying and Monitoring Potential Ecosystem Impacts of Geological Carbon Storage, Available from: http://www.bgs.ac.uk/qics/home/html

Rerolle, V.M.C., Floquet, C.F.A., Harris, A.J.K., Mowlem, M.C., Bellerby, R.R.G.J., Achterberg, E.P., 2013. Development of a colorimetric microfluidic pH sensor for autonomous seawater measurements. Anal. Chim. Acta 786, 124–131.

Song, Y.C., Nishio, M., Chen, B.X., Someya, S., Uchida, T., Akai, M., 2002. Measurement of the density of CO_2 solution by Mach–Zehnder interferometry. Vis. Imaging Transp. Phenom. 972, 206–212.

Statoil, 2013. Sleipner West, Available from: http://www.statoil.com/en/TechnologyInnovation/NewEnergy/Co2CaptureStorage/Pages/SleipnerVest.aspx

Svendsen, E., Saetre, R., Mork, M., 1991. Features of the northern North-Sea circulation. Cont. Shelf Res. 11 (5), 493–508.

Thomas, H., Bozec, Y., Elkalay, K., de Baar, H.J.W., 2004. Enhanced open ocean storage of CO_2 from shelf sea pumping. Science 304 (5673), 1005–1008.

Umlauf, L., Burchard, H., 2003. A generic length-scale equation for geophysical turbulence models. J. Mar. Res. 61 (2), 235–265.

Wakelin, S.L., Holt, J.T., Blackford, J.C., Allen, J.I., Butenschon, M., Artioli, Y., 2012. Modeling the carbon fluxes of the northwest European continental shelf: validation and budgets. J. Geophys. Res.: Oceans, 117.

Weiss, R.F., 1974. Carbon dioxide in water and seawater: the solubility of a non-ideal gas. Mar. Chem. 2 (3), 203–215.

Widdicombe, S., Blackford, J.C., Spicer, J.I., 2013. Assessing the environmental consequences of CO_2 leakage from geological CCS: generating evidence to support environmental risk assessment. Mar. Pollut. Bull. 73 (2), 399–401.